Detection of Sulfur-Related Defects in Sulfur Diffused n- and p-Type Si by DLTS

Katarzyna Gwozdz, Vladimir Kolkovsky,* Joerg Weber, Anastasia A. Yakovleva, and Yuri A. Astrov

Sulfur is diffused into Czochralski (CZ) and Float-Zone (FZ) silicon wafers at 1200 °C for 30 h. After diffusion, the wafers are slowly cooled in air. Several defect levels are observed by deep level transient spectroscopy (DLTS) in n- and p-type samples. All defects levels are related to sulfur defects, but none could be identified with the donor and double donor states of substitutional S or molecular S_2. Additional annealing of the samples at 300 °C generates four DLTS levels in n-type Si and no peaks in p-type Si. The enhancement of the emission rate with the electrical field confirm their donor and double donor-like behavior. The authors identify the four DLTS levels in the annealed n-type Si samples with the different charge states of monoatomic S and molecular S_2 (S^0, S^+, S_2^0, and S_2^+) defects in Si. Hydrogenation of the annealed samples by wet chemical etching results in a reduction of the intensity of S^0, S^+, S_2^0, and S_2^+ due to a passivation of these defects. The authors did not observe any electrically active SH-complexes in the hydrogenated samples.

1. Introduction

Recently, the enhanced absorption below the bandgap of highly sulfur doped Si (hyperdoping) initiated the development of highly sensitive photodetectors and found application in photovoltaics.[1–4] The control over S-related defects becomes an important task for reliable functioning of such devices. The electrical and structural properties of S defects in silicon have been investigated by electrical and optical measurements for almost 60 years.[5–11] Four energy levels of S-defects assigned to different charge states of isolated substitutional (S) and molecular

substitutional (S_2) sulfur were reported in refs. [12–14]. However, the level position of the defects varied from study to study.

Besides S and S_2 other shallow S-defects with an activation energies <0.1 eV were often reported in *n*-type Si.[9,11] The appearance of these shallow defects depends strongly on the processing conditions of the samples. Two sulfur-defects with activation enthalpies of 320 and 350 meV above the valence band were also reported in *p*-type Si.[12]

The interaction of S-defects with hydrogen was investigated in refs. [15–18]. Pensl et al.[15] reported a complete hydrogen neutralization of S-related defects by using the DLTS technique. Four DLTS peaks of S_2 and S were observed before hydrogenation whereas no DLTS signal was detected in the hydrogenated samples. Annealing of the samples at 500 °C restored the original defect concentrations. Infrared absorption and EPR measurements reported several SH-related donor complexes with binding energies in the range of 80–140 meV below the conduction band.[16,17]

In the present work we study defects in sulfur diffused *n*-and *p*-type Si by DLTS. Several S-defect levels could be observed directly after diffusion and slow cooling of the samples. After annealing the samples at 300 °C the number of DLTS levels was clearly reduced. In *n*-type Si only the levels of isolated S and molecular S_2 defects were detected. No defect level was detected in p-type Si after the anneal. Some of the defect levels in the diffused sample appear in the DLTS spectrum at the same position as the isolated double donors S and S_2. These levels could have been wrongly assigned to isolated and molecular sulfur in some previous studies. This might be an explanation of the large scatter in the electrical level positions of S and S_2 found in the literature.

2. Experimental Section

Two different Czochralski (CZ) silicon wafers with a doping level of about 6×10^{15} cm^{-3} (*n*-type) and 8×10^{15} cm^{-3} (*p*-type) and a single float-zone (FZ) Si wafer with a doping of about 5×10^{15} cm^{-3} (*p*-type) were intentionally doped with sulfur. The diffusion parameters for the S introduction were similar to those reported in ref. [19]. The diffusion temperature was 1200 °C and the diffusion time was 30 h. The sulfur vapor

K. Gwozdz
Department of Quantum Technologies
Faculty of Fundamental Problems of Technology
Wroclaw University of Science and Technology
Wybrzeze Wyspianskiego 27, 50-370 Wroclaw, Poland

Dr. V. Kolkovsky, Prof. J. Weber
Technische Universität Dresden
Institut für Angewandte Physik
01062 Dresden, Germany
E-mail: uladzimir.kalkouski@ipms.fraunhofer.de

Dr. A. A. Yakovleva, Prof. Y. A. Astrov
Ioffe Physico-Technical Institute
Russian Academy of Sciences
Politekhnicheskaya 26, St. Petersburg 194021, Russia

ADVANCED
SCIENCE NEWS
www.advancedsciencenews.com

physica
status
solidi
a
www.pss-a.com

pressure pressure in the ampoule was 0.05 atm. After the diffusion the wafers were cooled slowly in air. The samples of quadratic shape were cut from the wafers. Both *n*- and *p*-type Si samples were wet chemically etched (WCE) at room temperature (RT) in an acid consisting of HNO3:HF:CH3COOH with a volume ratio of 5:3:3. The etch removed a 50–70 μm layer from the surface. Schottky contacts were prepared by thermal evaporation of gold on *n*-type Si and aluminum on *p*-type Si at room temperature. Ohmic contacts were made by rubbing the back side of the samples with an eutectic InGa alloy. After the DLTS study of these samples, the contacts were removed, and the samples were annealed at 300 °C for 1 h in argon atmosphere. After a short HF-dip contacts were prepared as reported before.

Capacitance measurements were performed at a frequency of 1 MHz. DLTS and Laplace DLTS were used for the investigation of the electrical properties of deep traps. Laplace DLTS with two filling pulses was also employed to investigate the electronic properties (activation enthalpy and capture cross section) of deep levels and their depth profiles. The depth profiles of defects were determined from Laplace DLTS measurements at a fixed reverse bias and variation of two filling pulse biases. The lambda-layer was taken into account for the calculation of the depth profiles. From capacitance versus voltage measurements, the electrical field in the depletion layer of samples was determined as described in ref. [20]. The influence of the electric field on the emission rate was studied at fixed pulse biases while varying the reverse bias. We label the DLTS peaks according to electron (E) or hole (H) traps and the temperature of the maximal DLTS signal observed at an emission rate of 50 s^{-1}. In addition, we introduce an index S for the samples after WCE. In the annealed *n*-type sample we label the DLTS peaks according the identifications given in the literature.[8,11]

3. Results and Discussion

Figure 1 shows DLTS spectra recorded in *n*- and *p*-type Si for the S diffused sample after WCE (black curve). The red spectra are from the same samples after an additional anneal at 300 °C. Overall nine different DLTS peaks are observed in the WCE

n-type sample and three in the *p*-type sample. Annealing the sample at 300 °C leads to a significant reduction of the peak intensities or their disappearance. Four new DLTS peaks labeled S^0, S^+, S_2^0, and S_2^+ appear in the annealed *n*-type Si samples whereas only a broad band with a maximum at about 175 K was detected in the annealed *p*-type Si sample. Laplace DLTS measurements show that each DLTS peak observed in Figure 1 consists of a single line except the broad band in the annealed *p*-type Si sample. The Laplace DLTS spectrum of this defect depends strongly on the measurement conditions (the reverse bias, the bias of filling pulses, the width of the filling pulse and other) and could be related to extended defect states.

The activation enthalpy and the apparent capture cross section of the defects observed in Figure 1 was obtained from Laplace DLTS measurements. The Arrhenius plots are presented in **Figure 2** for *n*- and *p*-type Si, respectively. The black points show the Arrhenius plots obtained in the sample after WCE etching whereas the red points were determined from the annealed sample. The activation enthalpies and the apparent capture cross sections of the defects are combined in **Table 1**. Even if the Arrhenius plots of some levels in the WCE sample are very similar to those of S^0, S_2^+, or S_2^0 we will show later, that they belong to different defects.

In order to shed light on the origin of the defects detected in the WCE sample we determine their depth profiles (**Figure 3**). In the n- and p-type samples a decrease of the P or B concentration close to the surface, due to the formation of neutral boron-H or phosphorous-H complexes is observed. None of the levels in the WCE sample is descending toward the bulk of Si. Therefore, based on ref. [21] we could not correlate the defects observed after WCE to sulfur-hydrogen complexes. We find no identical profiles in the *n*- or *p*-type samples after WCE. This indicates that these levels cannot be assigned to different charged states of the same defect.

The depth profiles of S^0, S^+, S_2^0, and S_2^+ observed in the annealed *n*-type Si sample are shown in Figure 3(c). We found that the depth profiles of S^0 and S^+ as well as S_2^0 and S_2^+ are
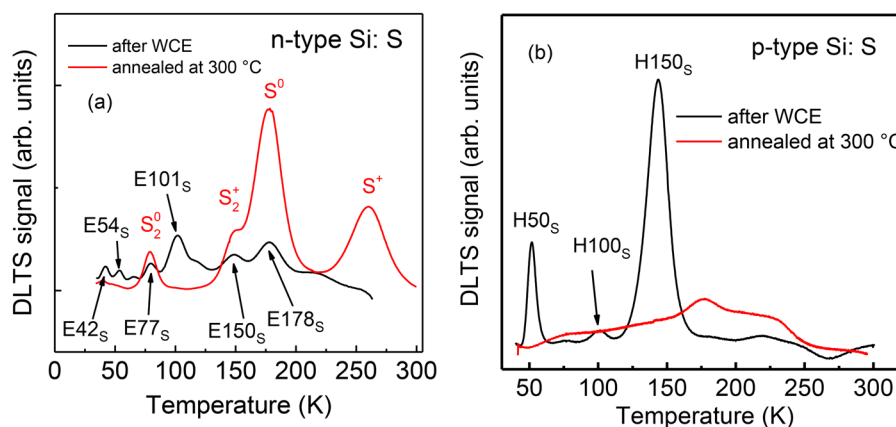

Figure 1. a) DLTS spectra recorded in *n*-type Si diffused with S: sample after WCE and after additional annealing at 300 °C; b) DLTS spectra recorded in *p*-type Si diffused with S: sample after WCE and after additional annealing at 300 °C. All spectra were recorded with a reverse bias of −2 V, a filling pulse of 0 V, and a rate window of 48 s^{-1}.
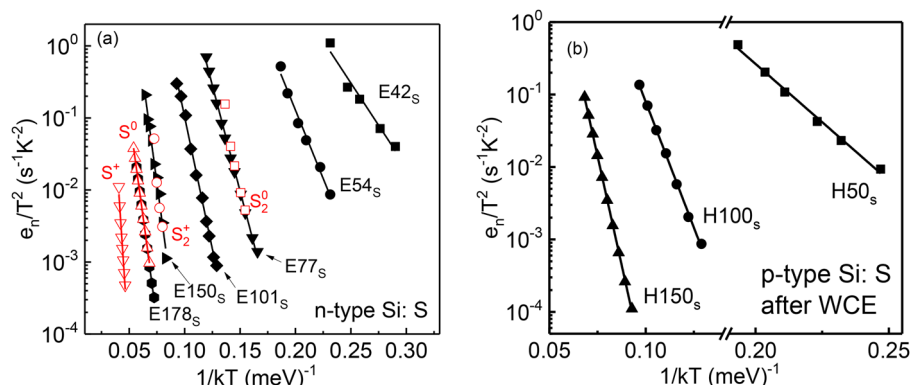
Figure 2. Arrhenius plots obtained from Laplace DLTS measurements in (a) *n*-type Si after WCE (black) and after annealing the samples at 300 °C (red) and in (b) *p*-type Si after WCE (black) and after annealing the samples at 300 °C (red).

within the experimental accuracy identical. Identical depth profiles of levels observed in the same sample after identical treatments indicate that both belong to the same defect. The depth profiles of S^0, S^+, S_2^0, and S_2^+ are descending toward the surface and this reduction may suggest a passivation by hydrogen, whose concentration increases close to the surface of samples.

In many cases the enhancement of the emission rate of defects with electric field can be related to the charge state of the defect. In the present study, we concentrate our attention only on the annealed sample. **Figure 4** plots the changes of the emission rate for S^0, S^+, S_2^0, and S_2^+ as a function of the square root of the electric field. Solid lines present results of a fit of the experimental points by using the 1D Poole–Frenkel model[22,23] for donors with a single charge state ($Z = 1$) or a double charge state ($Z = 2$). A good correspondence between experiment and theory was found for all defects investigated.

Table 1. Electrical properties (activation enthalpy and apparent capture cross section) of the sulfur-related levels determined from the Arrhenius plots in Figure 2.

Sample	Defects	$E-E_C$ or $E+E_V$ [eV]	σ_{na} [cm^2] or σ_{pa} [cm^2]
n-type after WCE	E42$_S$	54 ± 5	3×10^{-17}
	E54$_S$	87 ± 5	6×10^{-16}
	E77$_S$	135 ± 3	7×10^{-16}
	E101$_S$	168 ± 4	3×10^{-16}
	E150$_S$	248 ± 10	2×10^{-16}
	E178$_S$	266 ± 3	9×10^{-18}
n-type after additional anneal at 300 °C	S^0_2	154 ± 5	1×10^{-14}
	S^+_2	272 ± 29	1×10^{-15}
	S^0	257 ± 2	9×10^{-18}
	S^+	533 ± 28	3×10^{-15}
p-type after WCE	H50$_S$	74 ± 3	3×10^{-16}
	H100$_S$	160 ± 3	3×10^{-16}
	H150$_S$	277 ± 2	5×10^{-16}

The DLTS peaks in the *n*-type Si sample after WCE do not belong to molecular S_2 or atomic S. In spite of the similar electrical properties of E77$_S$, E150$_S$, and E178$_S$ with S_2^0, S_2^+, and S^0 the levels belong to different defects from the following arguments. Both single donor and double donor states of atomic S and molecular S_2 should always appear together. In the *n*-type WCE sample (Figure 1) no trace of a peak at the S^+ position was detected, whereas E178$_S$ which has similar electrical properties to S^0 was obviously observed in the DLTS spectrum. The apparent capture cross section of E77$_S$ and E150$_S$ differ significantly from those of S_2^0 and S_2^+. In our sample, E77$_S$, E150$_S$, and E178$_S$ were not observed after annealing at around 300 °C whereas the S and S_2-related defects only appear in the DLTS spectrum after annealing at such temperatures.

As mentioned above none of the defects observed in *n*- and *p*-type S-doped Si samples after WCE could be attributed to hydrogen related defects. We did not observe these defect levels in samples without S and therefore we identify all peaks in these samples to be S-related. The defects were not stable after heat treatments at about 300 °C. After annealing at such temperatures, the peaks disappear and four DLTS peaks labeled S_2^0, S_2^+, S^0, and S^+ were observed in the samples. As mentioned above, the depth profiles of S^0 and S^+ are identical. Similarly, identical depth profiles were observed for S_2^0 and S_2^+. These two defect levels were observed always together. The enhancement of the emission rate of the defects is consistent with the Poole–Frenkel model for single (S^0 and S_2^0) and double (S^+ and S_2^+) charged defects (see Figure 4). Therefore, we assign these defects to single donor and double donor states of atomic (S) and molecular (S_2) sulfur.

We did not observe any electrically active SH-related defects in *n*- and *p*-type samples after WCE. Generally, H is introduced into samples in its atomic form (positive or negative charge state) and it interacts easily with other crystal imperfections such as point or extended defects or interface states. The decrease of the concentration of the S-related centers toward the surface (Figure 3) could be correlated with the passivation of these electrically active defects by hydrogen in *n*-type Si. The absence of electrically active H-related defects in the samples after WCE support the findings of Pensl et al.[15,17] that H passivates
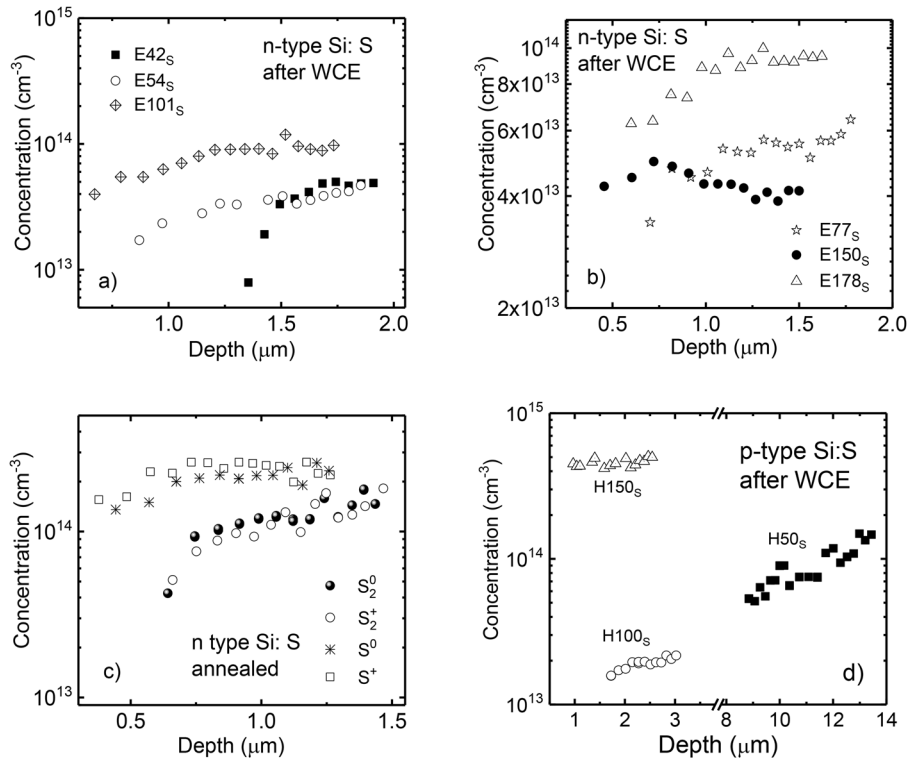
ADVANCED
SCIENCE NEWS
www.advancedsciencenews.com

physica
status
solidi
a
www.pss-a.com

Figure 3. Depth profiles of the traps observed in *n*- (a) and (b) and *p*-type (d) Si doped with S after WCE. The depth profiles of the traps after an additional anneal at 300 °C in *n*-type Si are shown in (c).
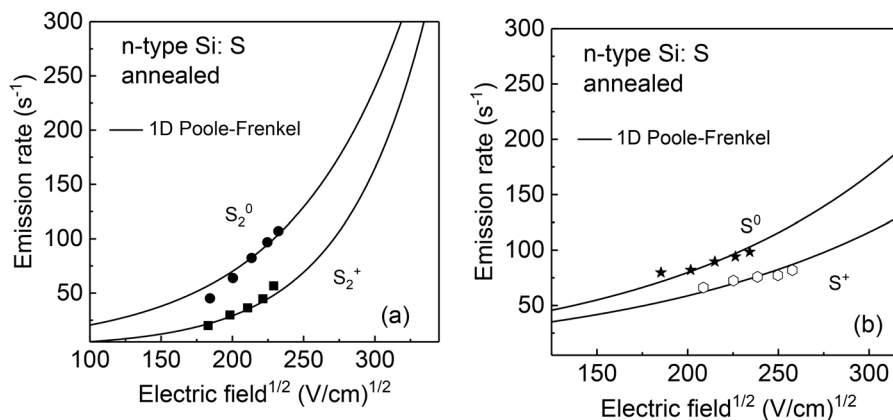

Figure 4. Emission rate versus the square root of the electric field recorded for S_2^0, S_2^+, S^0, and S^+ in annealed *n*-type Si doped with S.

molecular S_2 and S without the formation of other electrically active SH-related centers.

4. Conclusions

We observed a number of DLTS peaks in *n*-and *p*-type Si, which was diffused with S at 1200 °C. All peaks are related to different S-related defects. In the sample after WCE defect levels corresponding to the peaks ($E77_S$, $E150_S$, and $E178_S$) seem to be similar to those reported previously for the atomic and molecular sulfur defect. However, the analysis of the depth profiles and their thermal stability showed that the origin of the defects is different. Only annealing at 300 °C leads in our samples to the appearance of four DLTS peaks which can be identified with the donor and double donor levels of atomic S and molecular S_2. The enhancement of the emission rate of the defects is consistent with the Poole–Frenkel effect and confirms their donor- and double donor-like behavior. Hydrogenation of the annealed sample leads to a reduction of the concentration of the S and S_2 DLTS peaks, which is explained by a passivation of the donor and double donor states. No new electrically active SH-related defects were observed in a concentration above 10^{12} cm^{-3}.

Conflict of Interest

The authors declare no conflict of interest.

Keywords

[1] T.-H. Her, R. J. Finlay, C. Wu, E. Mazur, *Appl. Phys. A: Mater. Sci. Process.* **2000**, *70*, 383.
[2] K. C. Phillips, H. H. Gandhi, E. Mazur, S. K. Sundaram, *Adv. Opt. Photonics* **2015**, *7*, 684.
[3] J. F. Warrender, *Appl. Phys. Rev.* **2016**, *3*, 031104.
[4] G. Azzouzi, W. Tazibt, *Energy Proc.* **2013**, *41*, 40.
[5] N. Sclar, *J. Appl. Phys.* **1981**, *52*, 5207.
[6] R. O. Carlson, R. N. Hall, E. M. Pell, *J. Phys. Chem. Solids* **1959**, *8*, 81.
[7] G. W. Ludwig, *Phys. Rev.* **1965**, *137*, A1520.
[8] D. L. Camphausen, H. M. James, R. J. Sladek, *Phys. Rev. B* **1970**, *2*, 1899.
[9] S. D. Brotherton, M. J. King, G. J. Parker, *J. Appl. Phys.* **1981**, *52*, 4649.
[10] H. Pettersson, H. G. Grimmeiss, *Phys. Rev B* **1990**, *42*, 1381.
[11] H. G. Grimmeiss, E. Janzen, B. Skarstam, *J. Appl. Phys.* **1980**, *51*, 4212.
[12] G. Pensl, G. Roos, C. Holm, P. Wagner, *Mater. Sci. Forum* **1986**, *10–12*, 911.
[13] O. Engström, H. G. Grimmeiss, *J. Appl. Phys.* **1976**, *47*, 4090.
[14] W. E. Krag, W. H. Kleiner, H. J. Zeiger, *Phys. Rev. B* **1986**, *33*, 8304.
[15] G. Pensl, G. Roos, C. Holm, E. Sirtl, N. M. Johnson, *Appl. Phys. Lett.* **1987**, *51*, 451.
[16] I. S. Zevenbergen, T. Gregorkiewicz, C. A. J. Ammerlaan, *Phys. Rev. B* **1995**, *51*, 16746.
[17] R. E. Peale, K. Muro, A. J. Sievers, *Mater. Sci. Forum* **1991**, *65–66*, 151.
[18] G. Roos, G. Pensl, N. M. Johnson, C. Holm, *J. Appl. Phys.* **1990**, *67*, 1897.
[19] Y. A. Astrov, L. M. Portsel, A. N. Lodygin, V. B. Shuman, *Semicond. Sci. Technol.* **2011**, *26*, 055021.
[20] P. Blood, P. W. Orton, *The Electrical Characterization of Semiconductors: Majority Carriers and Electron States*. Academic Press, New York **1992**.
[21] O. Feklisova, N. Yarykin, *Semicond. Sci. Technol.* **1997**, *12*, 742.
[22] J. Frenkel, *Phys. Rev.* **1938**, *54*, 647.
[23] J. L. Hartke, *J. Appl. Phys.* **1968**, *39*, 4871.